PDXK mutations cause polyneuropathy responsive to PLP supplementation

Running head: Vitamin B_6-responsive CMT

Viorica Chelban MD, MSc[1, 2*], Matthew P. Wilson PhD[3#], Jodi Warman Chardon MD[4,5,6#], Jana Vandrovcova PhD[1#], M. Natalia Zanetti PhD[7], Eleni Zamba-Papanicolaou MD[8,9], Stephanie Efthymiou MSc[1], Simon Pope PhD[10], Maria R Conte PhD[11], Giancarlo Abis PhD[11], Yo-Tsen Liu PhD[12,13,14], Eloise Tribollet Ms[1], Nourelhoda A. Haridy MD[1,15], Juan A Botía PhD[16,17], Mina Ryten PhD[16, 18], Paschalis Nicolaou PhD[8,9], Anna Minaidou PhD[8,9], Kyproula Christodoulou PhD[8,9], Kristin D. Kernohan PhD[6, 19], Alison Eaton MD[6], Matthew Osmond MSc[6], Yoko Ito PhD[6], Pierre Bourque MD[4,5], James E.C. Jepson PhD[7], Oscar Bello PhD[7], Fion Bremner MD[20], Carla Cordivari MD[21], Mary M. Reilly MD, FRCP, FRCPI, PhD[1], Martha Foiani MSc[21,22], Amanda Heslegrave PhD[22,23], Henrik Zetterberg PhD[22,23,24, 25], Simon J.R. Heales PhD[10], Nicholas W. Wood PhD[1,26], James E. Rothman PhD[7,27], Kym M Boycott MD PhD[6], Philippa B. Mills PhD[3#], Peter T. Clayton PhD[3#] and Henry Houlden PhD[1,26*#] for the Care4Rare Canada Consortium[6] and the SYNaPS Study Group[28]

[1]Department of Neuromuscular Diseases, [7]Department of Clinical and Experimental Epilepsy, [16]Reta Lila Weston Research Laboratories, [22]Department of Neurodegenerative Disease, UCL Queen Square Institute of Neurology, University College London, London WC1N 3BG, UK.

[2]Department of Neurology and Neurosurgery, Institute of Emergency Medicine, Toma Ciorbă 1, 2052 Chisinau, Republic of Moldova.

[3]Genetics and Genomic Medicine, GOS Institute of Child Health, University College London, London WC1N 1EH.

[4]Department of Medicine (Neurology), University of Ottawa, [5]Ottawa Hospital Research Institute, [6]Children's Hospital of Eastern Ontario Research Institute, University of Ottawa, Ottawa, ON, K1H 8L1, Canada Ontario, Canada [19]Newborn Screening Ontario, Children's Hospital of Eastern Ontario, Ottawa, Canada.

[8]The Cyprus Institute of Neurology and Genetics, [9]Cyprus School of Molecular Medicine Nicosia, Cyprus.

[8]The Cyprus Institute of Neurology and Genetics, [9]Cyprus School of Molecular Medicine Nicosia, Cyprus.

[10]Neurometabolic Unit, [20]Neuro-ophthalmology Department, [21]Clinical Neurophysiology Department, [26]Neurogenetics Laboratory, National Hospital for Neurology and Neurosurgery, Queen Square, London, WC1N 3BG, UK

[11]Randall Centre of Cell and Molecular Biophysics, School of Basic and Medical Biosciences, King's College London, London SE1 1UL, UK

[12]Department of Neurology, Neurological Institute, Taipei Veterans General Hospital, [13]National Yang-Ming University School of Medicine, [14]Institute of Brain Science, National Yang-Ming University, Taipei, Taiwan

[15]Department of Neurology and Psychiatry, Assiut University Hospital, Faculty of Medicine, Assiut, Egypt

[17]Department of Information and Communications Engineering, University of Murcia, Campus Espinardo, 30100 Murcia, Spain

[18]Department of Medical & Molecular Genetics, King's College London, Guy's Hospital, SE1 9RT, London, UK

[23]UK Dementia Research Institute at UCL, London WC1N 3BG, UK

[24]Clinical Neurochemistry Laboratory, Sahlgrenska University Hospital, S-431 80 Mölndal, Sweden

[25]Department of Psychiatry and Neurochemistry, Institute of Neuroscience and Physiology, the Sahlgrenska Academy at the University of Gothenburg, S-431 80 Mölndal, Sweden

This article has been accepted for publication and undergone full peer review but has not been through the copyediting, typesetting, pagination and proofreading process which may lead to differences between this version and the Version of Record. Please cite this article as doi: 10.1002/ana.25524

[27]Department of Cell Biology, Yale School of Medicine, New Haven, CT 06520-8002, USA
[28]SYNaPS Study Group, see Supplemental data S6 for list of collaborators.
[#] These authors contributed equally to the work.
Key words: PDXK, polyneuropathy, optic atrophy, vitamin $B_{6,}$ pyridoxal kinase
Title: 88 characters, Running head: 25 characters
Word count: Abstract: 250, Introduction: 94, Discussion: 607, Body: 5508
Figures: 4 (colour figures 4), Tables: 3
***Correspondence to:** v.chelban@ucl.ac.uk and h.houlden@ucl.ac.uk

ABSTRACT

Objective: To identify disease-causing variants in autosomal recessive axonal polyneuropathy with optic atrophy and provide targeted replacement therapy.

Methods: We performed genome-wide sequencing, homozygosity mapping and segregation analysis for novel disease-causing gene discovery. We used circular dichroism to show secondary structure changes and isothermal titration calorimetry to investigate the impact of variants on ATP-binding. Pathogenicity was further supported by enzymatic assays and mass spectroscopy on recombinant protein, patient-derived fibroblasts, plasma and erythrocytes. Response to supplementation was measured with clinical validated rating scales, electrophysiology and biochemical quantification.

Results: We identified bi-allelic mutations in *PDXK* in five individuals from two unrelated families with primary axonal polyneuropathy and optic atrophy. The natural history of this disorder suggests that untreated, affected individuals become wheelchair-bound and blind. We identified conformational rearrangement in the mutant enzyme around the ATP-binding pocket. Low PDXK ATP-binding resulted in decreased erythrocyte PDXK activity and low pyridoxal 5'-phosphate (PLP) concentrations. We rescued the clinical and

biochemical profile with PLP supplementation in one family, improvement in power, pain and fatigue contributing to patients regaining their ability to ambulate during the first year of PLP normalization.

Interpretation: We show that mutations in *PDXK* cause autosomal recessive axonal peripheral polyneuropathy leading to disease via reduced PDXK enzymatic activity and low PLP. We show that the biochemical profile can be rescued with PLP supplementation associated with clinical improvement. As B_6 is a cofactor in diverse essential biological pathways, our findings may have direct implications for neuropathies of unknown aetiology characterised by reduced PLP levels.

INTRODUCTION

Peripheral neuropathies are amongst the most common neurological disorders worldwide affecting approximately 20 million people in Europe and USA alone with few disease-modifying treatments established for these conditions[1-3]. Inherited forms of peripheral neuropathies affecting both the motor and sensory nerves, known as Charcot-Marie-Tooth (CMT) disease, are the most common genetic neuromuscular disorders affecting approximately 1 in 2500 people[4-8]. However, only 25% of all autosomal recessive (AR) CMT cases have causal variants identified[9] and treatment is only supportive[1-3]. Most known genes associated with AR CMT cause disease either by affecting the cytoskeleton or axonal trafficking[2].

METHODS

Study participants

Patients with polyneuropathy and optic atrophy were identified by neurogeneticists at the National Hospital for Neurology and Neurosurgery London and The Children's Hospital of Eastern Ontario. The affected cases were recruited along with unaffected family members under IRB/ethics-approved research protocols (UCLH: 04/N034; CHEO: CTO/1577) with informed consent. All cases had extensive genetic, metabolic and mitochondrial investigations carried out that excluded acquired and other inherited causes of polyneuropathy and optic atrophy.

Phenotype and clinical measures

All cases had comprehensive phenotyping performed by neurogenetics specialists including clinical assessment, electrophysiology, neuroimaging and videography. Motor function was quantified using the Medical Research Council (MRC) muscle scale, a standardised scale for the assessment of peripheral nervous system that grades muscle power from 0 to 5 in six validated movements and provides a total score out of a possible 60 points. The disease severity and progression was assessed using validated Neurological Impairment Scale (NIS)[10] and the Charcot-Marie-Tooth neuropathy score 2 (CMTNS2). CMTNS2 is a reliable and valid composite of symptoms (three items), signs (four items), and neurophysiology (two items). It is designed to measure length-dependent motor and sensory impairment in genetic neuropathies[11; 12]. The NIS forms

part of the standard minimum dataset for the Functional Independence Measure and UK Functional Assessment Measure (UK FIM+FAM). It records severity of functional impairment (rated 0-3) across 13 domains mapped onto the International Classification of Functioning (ICF). The score range is 0-50. The affected individuals from family 1 had MRC scales, CMTNS2 and NIS assessment before and after replacement therapy.

Genome-wide sequencing and haplotype analysis

DNA was extracted from peripheral blood. Whole Genome Sequencing was performed by deCODE genetics, Inc. using DNA from the two affected siblings from family 1. Illumina HiSeq4000 instrument (Illumina, San Diego, CA, USA) was used to generate 100 bp paired-end reads. Alignment was performed using BWA (http://bio-bwa.sourceforge.net/)[13] with GRCH37 as a reference. Variants were called using the GATK [14-17] Unified Genotyper-based pipeline[14-16] workflow. All variants were annotated using ANNOVAR[18] and filtered using custom R scripts. Shared regions of homozygosity were identified using HomozygosityMapper[19] and Bcftools/RoH[20]. Only novel or very rare variants with a minor allele frequency (MAF) of < 0.01 in the 1000 Genomes Project[21], NHLBI GO Exome Sequencing[22], and Exome Aggregation Consortium database (ExAC)[23] were included. Coding/splicing, homozygous variants that were within the autozygome of the affected cases were prioritized.

Whole exome sequencing (WES) was performed in family 2 using DNA from both affected siblings and their mother as part of the Care4Rare Canada Consortium. Exonic DNA was selected using the Agilent SureSelect Clinical Research Exome V1 kit, then sequenced on an Illumina NextSeq 500 with 2x150bp chemistry. Read alignment, variant calling, and annotation were done as outlined for previous FORGE and Care4Rare Canada projects[24]. Average coverage for the exomes was 182x, 190x, and 244x and >97% of consensus coding sequences exons in all exomes were covered at >10×.

Sanger sequencing

The variants identified by WGS and WES were confirmed by Sanger sequencing. The region was amplified using the following primers: 5'-AGGAGGATCAGGGATGGGAG-3' and 5'-CTCTCATATCCTGCTCCCCA-3' in family 1 and 5'-CTTGCCGCTCTATGTTTGGAC-3' and 5'-GAGAGTGACAGGCGCAACTC-3' in family 2. The promoter region of *PDXK* was amplified using the following primers: 5'-GCGGTTCCCTTGGGTATC-3' and 5'-ACGCCTCCTTCTGACCTC-3'. Genomic DNA was extracted from dried blood spots from affected individuals from family 1 and controls using the QIAamp DNA Micro Kit and from blood from family 2. Sequencing reactions were performed using the BigDye Terminator 1.1 system (ThermoFisher, Paisley, UK) followed by sequencing using an ABI DNA Analyser (ThermoFisher, Paisley, UK). Electropherograms were analysed using the Sequencher software package (Gene Codes, MI, USA).

Gene co-expression analysis

We generated Gene Co-expression Networks (GCN) for CNS and PNS tissue-specific transcriptomic data generated by the Genotype-Tissue Expression Consortium[25] (GTEx7 V6 gene expression data accessible from https://www.gtexportal.org/). We analysed each of the tissue sample sets separately by filtering genes on the basis of an RPKM > 0.1 (observed in > 80% of the samples for a given tissue). We then corrected for batch effects, age, gender and RIN using ComBat[26]. Finally, we used the residuals of these linear regression models to construct gene co-expression networks for each tissue using WGCNA[27]and post-processing with k-means[28] to improve gene clustering. Gene modules were functionally annotated with gProfileR4 R package using the Gene Ontology (GO) database without Electronic Inferred Annotations (EIA) and accounting for multiple testing with gSCS[29]. The top down plot figure is done with Cytoscape 3.5.1[30]. We initially selected the 50 most connected genes within the black module, for the co-expression network of tibial nerve, based on adjacency values. We included all connections between genes. Then we filtered out the connections with weight <0.05. Finally, we applied a Kamada-Kawai layout algorithm to the remaining genes and edges to dispose them spatially at the canvas so their relative positions reflect similarity in connections.

Plasmid constructs

The human PDXK wild-type (WT) and PDXK mutant p.Ala228Thr cDNA were purchased from Invitrogen and cloned into the plasmid pGEX6p-1 (GE Healthcare, Piscataway, NJ) using the sites BamHI and NotI (New England Biolabs).

Protein purification

Escherichia coli strain Rosetta2 (DE3) (Novagen, Darmstadt, GER) was transformed with the plasmids pGEX6p-1-PDXK and pGEX6p-1-PDXK p.Ala228Thr and grown at 37°C to an OD_{600nm} of 0.8 and then induced with 0.5 mM Isopropyl β-D-1-thiogalactopyranoside (IPTG) for 4 hours. Cells were lysed, using a cell disruptor, (Avestin, Ottawa, CA) in lysis buffer containing 25 mM HEPES, pH 7.4, 400 mM KCl, 4% Trition X-100, 1 mM 1,4-dithiothreitol (Sigma-Aldrich) and SIGMAFAST™ Protease Inhibitor Cocktail Tablets, EDTA-Free (Sigma-Aldrich). The samples were supplemented with 5% polyethylamine (Sigma-Aldrich) and clarified using a 45Ti rotor (Beckman Coulter, Brea, CA) at 100,000 x g for 30 min prior to incubation overnight at 4°C with Glutathione Agarose beads (Pierce, Rockford, IL) previously washed in lysis buffer containing 1% Triton X-100. The Glutathione Agarose beads containing the immobilised proteins GST-PDXK and PDXK p.Ala228Thr were subsequently washed in lysis buffer containing 1% Triton X-100 and incubated with 10mg/ml DNAse and RNAse (Sigma-Aldrich) for 1 hour at room temperature (RT), prior to washing in lysis buffer containing no Triton X-100. The GST tag was cleaved using 100 U of PreScission Protease (GE Healthcare, Piscataway, NJ) for 2 hours at RT. After elution the proteins were dialyzed in 25 mM HEPES, pH7.4, 100 mM

KCl, 1mM 1,4-dithiothreitol overnight at 4°C. Protein concentration was determined using the BCA Protein Assay Kit (Thermo Fisher Scientific).

Circular dichroism (CD)

To investigate conformational differences between wild-type PDXK and the disease-linked mutant p.Ala228Thr, circular dichroism (CD) analyses were performed. The extinction coefficients of both proteins (ε_{280} = 31400 $M^{-1}cm^{-1}$) were calculated using the ProtParam tool within the ExPASy Portal[31]. Proteins were prepared as described above and dialysed overnight at 4°C in 30 mM TRIS pH 7, 100 mM KCl, 3 mM $MgCl_2$, 0.5 mM TCEP. Samples were concentrated to 0.2 mg/mL using Amicon Ultra-0.5 mL centrifugal filters (Merck).

UV and CD spectra were acquired on the Applied Photophysics Ltd Chirascan Plus spectrometer across the 400-190 nm wavelength region. 10 mm (400-230 nm) and 0.5 mm (260-190 nm) strain-free rectangular cells were employed. The instrument was flushed continuously with pure evaporated nitrogen throughout the experiment. The following parameters were employed: 2 nm spectral bandwidth, 1 nm step-size and 1 s instrument measurement time-per-point. All spectra were acquired at 25°C, and buffer baseline corrected. Light scattering correction was applied on the UV spectra of both proteins using the Chirascan Pro-Data Software (APL). Where possible, spectra were smoothed with a window factor of 4 using the Savitzky-Golay method[32] for better presentation.

The far-UV CD spectra of the two proteins were corrected for concentration and pathlength and expressed in terms of Δε ($M^{-1}cm^{-1}$) per amino acid residue. Protein secondary structure content was assessed using the Principle Component Regression method based on 16 known protein structures[31] embedded in the PLSPlus/IQ routine on the GRAMS32 AI software (Galactic, USA).

Isothermal titration calorimetry (ITC)

The affinity of a non-hydrolysable analogue of ATP, called Adenosine 5'-(3-thiotriphosphate) tetralithium salt (ATPγS), for both PDXK WT and p.Ala228Thr mutant, was examined using a MicroCal Isothermal Titration Calorimeter ITC200 instrument (Malvern). Both proteins were prepared as described above in 30 mM TRIS pH 7, 100 mM KCl, 3 mM $MgCl_2$, 0.5 mM TCEP (ITC buffer). An initial 0.2 M stock of ATPγS was prepared in water and diluted with ITC buffer to a final concentration of 250 µM. The concentration was adjusted using the UV Absorbance at 259 nm, and the extinction coefficient of 15.4 $mM^{-1}cm^{-1}$ suggested by the ligand provider (Jena Bioscience).

The experiments were conducted at 25°C following standard procedures as described previously[33]. 40 µL of 250 µM ATPγS was titrated into a 330µL solution of 25 µM WT or p.Ala228Thr protein. The ITC experiment consisted of twenty 2µL injections with a spacing of 180 seconds. Heat produced by titrant dilution was obtained by a control experiment, titrating into buffer alone, under the same conditions.

The MicroCal-Origin 7.0 software package was used to fit the integrated heat data obtained for the titrations corrected for heats of dilution, using a non-linear least-squares minimization algorithm based on an independent binding sites model. ΔH (reaction enthalpy change in kcal/mol), Ka ($1/K_D$) (equilibrium association constant per molar) and n (molar ratio of the proteins in the complex) were the fitting parameters. The reaction entropy was calculated using the relationships $\Delta G = \Delta H - T\Delta S = -RT\ln(1/K_D)$.

Western blotting

Fibroblast samples from affected, carriers and healthy people were obtained with consent. After reaching 90% confluence, the cultured cells were harvested and lysed in ice cold lysis RIPA buffer containing 50mM Tris-HCl pH 8.0, 150mM NaCl, 0.5% DOC, 0.1% Triton X-100, 0.1% sodium dodecyl sulphate (SDS) and SIGMAFAST Protease Inhibitor Cocktail for 30 minutes. The lysate was then centrifuged at 16000 g at 4°C and the supernatant transferred to a new tube. The protein concentration was measured using the BCA protein assay kit (Pierce) according to manufacturer's protocol. Equal amounts of protein (30 µg) from affected and healthy individuals were separated on a 10% SDS-PAGE gel (NuPAGE Invitrogen) and transferred onto an Immobilon membrane (Millipore). After blocking the membrane with 2% fat free milk in PBS-Tween for 1 hour at RT, the membrane was incubated with anti-PDXK antibody (Abcam 38208; 1:500) for 1 hour at RT. The membranes were subsequently washed and incubated with horseradish peroxidase conjugated goat anti rabbit IgG (17210, Bio-Rad Laboratories, 1:5,000) for 1h

at RT. Blots were developed using ECL Prime (GE Healthcare), visualized via a ChemiDoc Touch Imaging System and analysed using Image Lab 5.2 software (Bio-Rad Laboratories). For the quantification, the signal intensity of each band corresponding to the PDXK WT and PDXK p.Ala228Thr mutant protein were normalized to the signal intensity of the corresponding reversible Ponceau staining as a reliable loading control[34]. The amount of PDXK WT and mutant protein were expressed as a percentage of the control sample. The experiment was repeated 3 times.

Measurement of pyridoxal kinase activity

The pyridoxal kinase activity present in dried blood spots (DBS) was determined by adapting the protocol used by Wilson *et al*[35] with the following modifications. 3 mm discs punched from dried blood spots were incubated for 10 min at 37 °C with shaking at 300 rpm in a reaction buffer containing 20 mmol/L potassium phosphate adjusted to pH 6.1, 10 µmol/L pyridoxal and 300 µmol/L MgATP (all purchased from Sigma-Aldrich, Gillingham, UK). The same method was adapted for the investigation of activity of the purified recombinant pyridoxal kinase. 5 µl of 20 ng/µl purified pyridoxal kinase protein lysate was placed in a UPLC 96-well sample plate (Waters, Elstree, UK). Subsequently, 115 µl of reaction buffer containing potassium phosphate (pH 6.1), pyridoxal and MgATP was added to create a final concentration of 20 mmol/L potassium phosphate, with pyridoxal and MgATP concentrations adjusted as appropriate. Investigation of pyridoxal kinase kinetics as a function of pyridoxal concentration used a MgATP concentration of 300

µmol/L. A pyridoxal concentration of 50 µmol/L was utilised for the determination of pyridoxal kinase kinetics as a function of MgATP concentration. After reaction buffer addition, the plate was incubated for 10 min at 37 °C in an Eppendorf Thermomixer C with shaking at 300 rpm prior to addition of 120 µl of a reaction stop mix identical to that used for the determination of pyridoxamine 5'-phosphate oxidase activity from dried blood spots.

Dried blood spots (DBS) were collected from 4 affected cases and 22 controls (age 15 – 92). Pyridoxal kinase activity of the recombinant proteins and that of dried blood spots was determined by using liquid chromatography-tandem mass spectrometry (UPLC-MS/MS) to determine the formation of pyridoxal 5'-phosphate after incubation of these with the enzyme substrate pyridoxal and expressed as µmol PLP L^{-1} h^{-1} from recombinant protein and as pmol PLP (3 mm DBS)$^{-1}$ h^{-1} from dried blood spots.

Data collection and statistical analysis were performed using Waters MassLynx and GraphPad Prism 6.0 software packages.

UPLC-MS/MS measurement of the B_6 vitamers

B_6 vitamer concentrations (pyridoxine (PN), pyridoxal (PL), PLP, pyridoxamine (PM), pyridoxamine phosphate (PMP)) and pyridoxic acid (PA) were quantified by ultra performance liquid chromatography-tandem mass spectrometry (UPLC-MS/MS) using stable isotope-labelled internal standards[35; 36].

HPLC measurement of B_6 vitamers

Pyridoxal phosphate was measured by HPLC with fluorescence detection using a Chromsystems kit as described previously[35]. Pyridoxic acid concentration was calculated using an external calibration standard.

PLP measurements pre and post PLP-replacement

Plasma PLP concentrations pre- and post PLP replacement were measured using two independent HPLC and UPLC-MS/MS methods as described above to validate the results. The difference between groups was tested with the use of a one-way analysis-of-variance test, followed by Tukey-Kramer Test. The middle lines of the bars indicate mean values, ±1 SD.

Measurement of neurofilament light chain (NFL) concentration

Plasma NFL concentration was measured by digital enzyme-linked immunosorbent assay using the commercially available NF-Light kit on a Single molecule array (Simoa) platform (HD-1 Analyzer) according to instructions by the manufacturer (Quanterix, Lexington, MA). All measurements were performed in duplicates, in one round of experiments using one batch of reagents. Intra-assay coefficients of variation were <10%.

RESULTS

Here we describe five affected cases from two unrelated families (Figure 1A) with early, childhood-onset sensorimotor, length dependent, predominantly axonal polyneuropathy and adult onset optic atrophy (Table 1).

Disease characterization

Family 1 is of Cypriot origin (affected individuals F1-II-5, currently 80 years, F1-II-6, currently 75 years and F1-II-9 died at 71 from an unrelated medical condition). Three affected siblings presented with difficulties running, distal wasting and weakness in the lower limbs before the age of 10 years, progression to upper limbs by age of 12 and onset of visual loss in their 40s. The disease progressed and at age of 79, case F1-II-5 required the assistance of two people for sit-to-stand, mobilising with the assistance of two plus zimmer-frame for transfers and short distances, and using a wheelchair for all other activities. Neurogenic-type pain, particularly in the lower limbs, was difficult to control despite multiple lines of symptomatic treatment. Case F1-II-6 (age 74) could only walk short distances with assistance from one individual. Neurological examination showed bilateral distal wasting from mid forearm and below the knee, with wasting of the thenar, hypothenar, intrinsic muscle of the hands, distal lower limbs muscles, *pes cavus*, and absent reflexes throughout in both patients (Figure 1B). The MRC muscle score was 44 (of 60) in case F1-II-5 and F1-II-6. Strikingly, both patients had severely reduced sensation in

all limbs and in all modalities with profound joint position sense loss up to the knee and vibration loss up to the iliac crest in both cases (Table 1 and Supplemental data S1). Vision was reduced (including colour vision) and fundoscopy confirmed bilateral optic atrophy in both cases (Figure 1C). The remaining cranial nerve examination was normal. The third sibling F1-II-9 (now deceased) was similarly affected.

Family 2 is of Scottish (paternal) and Italian (maternal) origin with two affected sisters (patient F2-II-1, currently 31 years; patient F2-II-2, currently 29 years) who presented with childhood-onset of a mild decrease in balance, which progressed to difficulty with running in adolescence, and progression to mild distal hand weakness the 3rd decade. Both sisters ambulate independently without aides and neither sister has symptoms of visual loss at their present ages. Neurological examination showed mild symmetrical distal wasting in hand intrinsic muscles and prominent distal lower limbs muscle wasting with *pes cavus* and mild hammertoes. There was mild distal weakness in hand intrinsics in the upper limbs and in the toes and distal lower legs and feet. The MRC scores were 56 (F2-II-1) and 54 (F2-II-2). Both sisters were areflexic, with reduced pinprick in the lower extremities and decreased vibration to the knees (Table 1 and Supplemental data S1). Colour vision was reduced. Fundoscopy confirmed bilateral optic atrophy in both cases; the remainder of the cranial nerve examination was normal.

Nerve conduction studies (NCS) in all affected cases revealed a progressive length-dependent, sensorimotor, predominantly axonal neuropathy (Supplemental data S2). Early in the disease (as seen in family 2) the NCS show a predominantly axonal neuropathy affecting mainly the lower limbs with absent sensory responses. Mild conduction slowing with normal motor responses was recorded in the upper limbs. The natural history of this disorder in the older individuals from family 1 (F1-II-5 and F1-II-6) with data recorded over 20 years of disease duration suggests that untreated, the neuropathy progresses in a length-dependent fashion and is characterised by prolonged DMLs, severe reduction of CMAPs in addition to absent sensory responses affecting upper and lower limbs as confirmed on NCS. Interestingly, both patients present with significantly more prolonged DML in the median compared to ulnar nerve (6.1 vs 3.6 ms). While it is possible that this is secondary to long-standing median compression lesion at the wrist we cannot exclude that this finding is disease-related. The reduced CMAPs were associated with reduction of conduction velocities in the intermediate range mainly in the median nerves. Electromyography in all cases tested was consistent with chronic denervation with no myopathic changes.

To further ascertain the exact type of neuropathy we performed a nerve biopsy in case F1-II-6. It showed diffuse and severe depletion of both small and large myelinated axons with regenerating clusters but no “onion bulbs”. This confirms a long-standing axonopathy with no overt demyelination (Figure 1D).

All cases reported here had pale optic discs on clinical examination. We performed visual evoked potentials (VEPs) to further describe the involvement of the optic nerve in the course of disease. We found that VEPs in case F1-II-6 have decreased considerably in amplitude from 7.9 and 7.4 in each eye to 1.8 and 1.9 over 20 years period indicating axonal loss and bilateral visual pathway involvement (Supplemental data S2). Similar results were confirmed in case F1-II-5. Family 2 has not been investigated with VEPs.

Identification of disease-causing PDXK variants

Previous extensive genetic[37], metabolic and mitochondrial investigations failed to identify any acquired, or known causes of inherited polyneuropathy in all cases. Whole genome sequencing (WGS) and homozygosity mapping in family 1 revealed a homozygous region on chromosome 21 with a shared region from 42-45 Mb on chromosome 21. This region included a shared homozygous variant in the two affected siblings that was carried by unaffected family members in heterozygous state: *PDXK* (NM_003681) c.682G>A (p.Ala228Thr). This variant was absent in 150 Cypriot controls. p.Ala228Thr is absent from the gnomAD database in homozygous state though reported in 7 heterozygous alleles (5 South Asian and two European) from 250586 (total allele frequency of 0.00002793)[23].

Independently, homozygosity mapping in family 2 revealed a 1.35Mb region of homozygosity on chromosome 21. WES in family 2 identified a shared homozygous

variant in this region, the c.659G>A p.(Arg220Gln) in the two affected sisters and was carried by each parent. This variant is absent from gnomAD in homozygous state and reported in 5 heterozygous European alleles from 250146) (total allele frequency of 0.00001999)[23]. It is predicted to be deleterious to protein function by *in-silico* programs (Combined Annotation Dependent Depletion (CADD) score 24). Sanger sequencing in affected individuals and carriers confirmed both variants (Figure 1E).

PDXK is ubiquitously expressed in humans encoding for pyridoxal kinase (PDXK), a cytoplasmic protein that converts vitamin B_6 to its active form, pyridoxal 5'-phosphate (PLP) (Figure 1F). PLP is an essential cofactor for >70 human enzymes representing diverse, essential biological pathways including amino acid and neurotransmitter metabolism.

Since *PDXK* mutations produce a peripheral rather than a predominantly central nervous system disease we investigated these differences further *in-silico* using public bulk tissue[25] and cell-specific transcriptomic data[38]. This demonstrated that human peripheral (tibial – mixed motor and sensory) nerve is amongst the tissues with the highest expression of *PDXK* (Figure 2A) with evidence for expression specifically in peripheral sensory neurons, based on single cell mouse transcriptomic data[38] (Figure 2B). This showed different co-expression profiles in brain compared to peripheral nerve tissue. Weighted gene co-expression analysis demonstrated that in 9 of 11 brain regions

analysed *PDXK* was co-expressed with genes relating to synaptic transmission and neuronal identity whilst co-expression data from the tibial nerve showed that *PDXK* was located within a module enriched for genes involved in oxidation-reduction processes (GO:055114, FDR-corrected p-value = 2.36×10^{-9}) (Figure 2C and Supplemental S3).

Assessment of the impact of PDXK variants on protein structure and enzymatic activity

Arginine 220 and Alanine 228 are evolutionary conserved amino acids in eutherians (Figure 2D). Arginine 220 is located in the β9 in the vicinity of the ATP binding site[39]. Alanine 228 is located in the ATP-binding pocket of pyridoxal kinase (Figure 2E) a critical region of the kinase, part of the loop region between strand β11 and helix α7 that rotates away from the active site allowing binding of the ATP adenine[39]. Whilst the Ala228 side-chain does not contact ATP directly, its backbone is involved in recruiting ATP to the catalytic pocket.

Far-UV circular dichroism (CD) spectra analysis of both WT and p.Ala228Thr revealed that, whilst both proteins were folded, there were small but significant differences in their secondary structure (Figure 3A). WT PDXK had an estimated α-helix and β-strand content of 31.2% and 19% respectively; similar to previous X-ray studies (PDB 3KEU)[40]. In the mutant protein a 26.0% and 21.1% of helical and strand content, respectively, was estimated, suggesting altered protein conformation. Furthermore, near-UV CD analysis revealed distinctive CD fingerprints for wild-type and p.Ala228Thr proteins, indicating

conformational rearrangements of aromatic side-chains[41] around the catalytic pocket, most likely hindering the enzyme's ability to bind ATP.

We performed isothermal titration calorimetry (ITC) confirming that p.Ala228Thr affected the ATP-binding ability of PDXK. Interaction of wild-type (WT) PDXK with the non-hydrolysable ATP analogue ATPγS generated well-interpolated, sigmoid-shaped curves, based on an independent and equivalent binding sites model centred on 1:1 stoichiometry. By contrast, no association between p.Ala228Thr and ATPγS was observed (Figure 3B).

Whilst no reduction in the expression of the mutant protein (p.Ala228Thr) compared to wild-type PDXK in case-derived fibroblasts was evident (Figure 3C), kinetic studies with human recombinant PDXK showed an approximate two-fold increase in the K_m of the p.Ala228Thr mutant protein (31.9 µmol/L) for pyridoxal compared to wild-type protein (14.5 µmol/L) and a reduction in the V_{max} of the mutant protein (p.Ala228Thr) to 0.95 µmol L^{-1} h^{-1} compared to 2.52 µmol L^{-1} h^{-1} for wild-type PDXK. Upon variation of MgATP concentration, sigmoidal kinetics were observed (WT $k_{0.5}$ = 53.4 µmol/L; V_{max} = 16.8 pmol h^{-1}, p.Ala228Thr $k_{0.5}$ = 174.4 µmol/L; V_{max}= 6.3 pmol h^{-1}) indicating cooperative binding between the two substrates, ATP and pyridoxal (Figure 3D-E).

Analysis of erythrocyte PDKX activity from cases carrying the p.Arg220Gln and p.Ala228Thr substitutions further confirmed the deleterious effect of these variants on pyridoxal kinase activity (Figure 3F). The PDKX activity in the 4 affected cases was reduced (1.1 and 0.8 pmol $DBS^{-1}\,h^{-1}$ in family 1 and 1.19 and 0.5 pmol $DBS^{-1}\,h^{-1}$ in family 2) relative to controls (2.6–14.7 pmol $DBS^{-1}\,h^{-1}$, mean; 8.0). Heterozygote activity (n=1, F-1-III-1) was within normal range (4.9 pmol $DBS^{-1}\,h^{-1}$). No correlation of DBS pyridoxal kinase activity with age was identified in controls. When segregated according to gender, a difference was identified between control males and females (9 male: mean=9.2 range=5.9-14.7; 12 female: mean=7.1 range=2.6-11.7) that approached significance (P = 0.1099 by untailed T test). An insertion located in the erythyroid-specific promoter region of pyridoxal kinase has been associated with reduced erythrocyte PDXK activity[21]. Sequencing this region showed that the reduced activity of all affected individuals was not attributable to this insertion [42] (Supplemental S4).

Finally, we measured plasma PLP concentrations in all affected individuals. Plasma PLP was greatly reduced in cases carrying the p.Arg220Gln and p.Ala228Thr compared to age-matched controls (Figure 3G-H).

In order to quantify the axonal damage we measured the neurofilament light chain (NFL) protein in plasma from patients carrying *PDXK* mutations. NFL, a major axonal cytoskeletal protein, is released into cerebrospinal fluid (CSF) and blood during axonal

breakdown[43] providing a dynamic biomarker of axonal damage in neurodegenerative disorders, including inherited neuropathies[44]. Both p.Arg220Gln and p.Ala228Thr variants were associated with high NFL (case F2-II-1: 49.6 pg/mL and in case F1-II-5: 25 pg/mL), within the range of NFL concentrations published for other axonal CMTs[44].

Supplementation with PLP is associated with biochemical correction and clinical improvement

Based on clear pathogenicity of the *PDXK* mutation leading to low PLP, case F1-II-5 and F1-II-6 were treated with oral PLP. High doses of pyridoxine are known to be neurotoxic[45], therefore we used PLP, which is hydrolysed to PL, to increase the upstream pyridoxal and force the flux with an enzyme with a high K_m based on our results of recombinant p.Ala228Thr protein kinetics. We initiated PLP replacement with 50 mg/day PLP, a dose that was commonly used in adults taking pyridoxal 5'-phosphate as a vitamin supplement with no reported side effects. We aimed to achieve plasma PLP concentration above the normal range by PLP replacement and this was achieved with 50 mg/day.

Two weeks after initiating the supplementation, plasma PLP levels had increased considerably without any side effects. PLP levels remained stable at 1, 3, 12, 18 and 24 months on PLP replacement (Figure 4A-B, Table 2) with improvement in symptoms (Supplemental data S5). Clinical improvement was noted after the first 3 months of PLP

replacement in the absence of any additional physiotherapy. Sensory examination and vision remained unchanged in both cases. Main motor improvements were in elbow and wrist flexion/extension and hip and knee flexion/extension with modest improvement in finger extension (Supplemental data S1) leading to 8 and 6 points improvement in the MRC sum score at 18 months on PLP replacement in case F1-II-5 and case F1-II-6, respectively. At last examination, 24 months on PLP replacement, patients were ambulating with high-stepping gait, unaided (Video 1). Furthermore, neuropathic pain has completely subsided; neither case requires additional analgesic medication.

These results led to an improvement of 5 points in the Neurological Impairment Set (NIS) score in case (F1-II-5) and the 4 points in case F1-II-6 based on motor, pain and fatigue subsets. Similarly, the CMT neuropathy score on PLP replacement improved by 4 points and 2 points in case F1-II-5 and F1-II-6 respectively (Supplemental data S5).

Electrophysiology studies performed 18 months after PLP supplementation have demonstrated no disease progression with no significant changes in the motor and sensory responses. Whilst the distal motor responses are not significantly different from previous studies, the EMG of the proximal muscles shows motor unit recruitment and interference pattern improvement in the proximal muscles (quadriceps and tibialis anterior muscles, biceps and flexor carpi radialis) with activity present in the tibialis anterior that was un-recordable on previous studies.

The clinical response to PLP replacement was further supported by measuring neurofilament light chain (NFL) protein in pre- and post- PLP replacement plasma from the *PDXK* cases in family 1. A reduction of NFL levels to the normal control range[44] (median 13 pg/mL, range 11-18 pg/mL) (Figure 4C) occurred upon restoration of PLP levels and continued to improve with PLP supplementation. At 24 months with PLP supplementation, the NFL level was 2.5 times lower than before supplementation.

DISCUSSION

Here we show that bi-allelic mutations in *PDXK* lead to peripheral neuropathy with optic atrophy. We have shown previously that several inherited disorders affecting B_6 vitamer metabolism, or resulting in inactivation of PLP, are implicated in neurological conditions. These include PNPO-(MIM: 603287)[46], ALDH7A1-(MIM: 266100)[47; 48] and PROSC-deficiency (MIM: 604436)[49; 50] where the lack of PLP in the brain leads to early onset, vitamin B_6-dependent epilepsy refractory to anticonvulsants. In most cases, delayed vitamin B_6 supplementation results in early death or severe handicap in these disorders. The PDXK activity is tissue-specific under PLP-deficiency conditions. In rats, B_6 deficiency leads to rapid decreases in PDXK activity in the peripheries (liver, muscle and plasma) with maintained PDXK activity and B_6 supply in the brain[51; 52]. This could explain the absence of seizures in humans with PDXK deficiency that present predominantly with peripheral nerve disease and normal CNS function. Furthermore, our *PDXK* co-expression networks analyses from peripheral nerve suggest a link to a module enriched for genes involved in oxidation-reduction processes in which mitochondria plays a significant role. PLP is a cofactor for several mitochondrial enzymes, but it is not certain how PLP is transported into mitochondria in humans; in yeast there is evidence for involvement of Mtm1p[53]. Whilst we acknowledge that co-expression networks generated from bulk RNA-seq of peripheral nerves are complex to interpret, there is growing evidence for the presence and importance of axonal RNA transport[54-56]. Thus, our findings are interesting given the strong phenotypic similarity (optic atrophy and axonal polyneuropathy) to

other disorders caused by mutations in genes involved in mitochondrial functions associated with neurodegeneration such as *OPA1* (MIM: 605290), *DHTKD1* (MIM: 614984), *MFN1* (MIM: 608506) and *MFN2* (MIM: 608507). Interestingly, within the *PDXK* regulon from the tibial nerve we found *DHTKD1* already linked to Mendelian disorders and associated with primary peripheral axonal neuropathy[57; 58]. This data suggests that within this regulon there may be other genes involved in neuronal maintenance that could cause a similar disease phenotype to be discovered.

Clinically, the *PDXK*-related neuropathy presented with mixed sensory and motor involvement in early childhood and was associated with optic atrophy later in adulthood. Electrophysiologically, one of the earliest signs of the disease was the absence of sensory responses even when the motor responses were within normal limits as seen in family 2. We note that the patients with longstanding disease (family 1) had significant standing and walking difficulties despite a mild proximal motor deficit most likely due to the combination of severe distal motor involvement with severe proprioceptive impairment extending to the proximal joints exacerbated by the severely impaired vision[59].

Based on our collective experience in rare diseases, we acknowledge that it is very difficult to implement randomized case-control studies for these patients and the subsequent limitations when designing therapeutic interventions. We would like to note that some clinical improvements seen in the patients reported here, such as pain and fatigue, are susceptible to placebo effects. Furthermore, the severity of the

polyneuropathy in the cases that received PLP supplementation and the absence of more proximal nerve-conduction studies is a limitation for the characterization of the neurophysiological phenotype and response to treatment. However, whilst we are limited in our ability to fully explain the mechanism of clinical improvement the supplementation with PLP was associated with normalization of the biochemical profile and improved clinical outcomes in individuals F1-II-5 and F1-II-6. The clinical improvement was supported by the normalisation of PLP levels, stable electrophysiological picture and NFL normalisation after treatment. Furthermore, animal models of *PDXK* knockdown, B_6 dietary deficiency and pharmacological models, all showed significant decreases in circulating PLP levels with reversible adverse effect(s) on the peripheral/sensory nerve similar to the human phenotype observed here (Table 3). The severe sensory involvement recorded at least 20 years before treatment, most likely accounted for the absence of a clinical effect on the sensory function in the two patients from family 1. We are limited in our ability to fully quantify the potential for electrophysiological improvement at this stage in the disease due to severe axonal loss, short interval of PLP replacement and the absence of more proximal nerve-conduction studies. Therefore, larger studies with treatment started earlier in the disease are warranted in order to assess the full potential benefit from treatment.

Conclusion

We show that bi-allelic mutations in *PDXK* cause autosomal recessive axonal peripheral polyneuropathy leading to disease via reduced PDXK enzymatic activity and low PLP. We show that the biochemical profile in affected individuals can be rescued with PLP supplementation and that this is associated with improvement in clinical scales. Therefore, we recommend that *PDXK* mutations should be screened for in patients with autosomal recessive, early-onset polyneuropathy and supplementation with PLP should be started promptly with long-term monitoring of clinical outcomes. Furthermore, B_6 vitamers can be linked to diseases through a wide-range of processes and genes involved in the vitamin B_6 pathway. Therefore, our results can be extended to other neuropathies of different aetiology characterised by reduction of PLP levels or reduction of PLP-dependent enzyme activities. Collectively, these data expand the genetic causes of primary polyneuropathy and the heterogeneity of inborn errors of vitamin B_6 metabolism and identifies PLP as a potential therapeutic target for this disorder.

Acknowledgements

The work on family 1 was supported by The Wellcome Trust (Synaptopathies strategic award (104033)), a Wellcome Trust Multi-User Equipment Grant, Muscular Dystrophy UK (MD UK), MDC USA and The Medical Research Council (MRC UK International Centre and project grants). The work on family 2 was performed under the Care4Rare Canada Consortium funded by Genome Canada and the Ontario Genomics Institute (OGI-147), the Canadian Institutes of Health Research, Ontario Research Fund, Genome Alberta, Genome British Columbia, Genome Quebec, and Children's Hospital of Eastern Ontario Foundation. ITC and CD experiments were carried out at the Centre for Biomolecular Spectroscopy, King's College London, established with a Capital Award from the Wellcome Trust (085944/Z/08/Z and 085944/B/08/Z). We thank Tam Bui for assistance with running CD experiments and Henny Wellington for assistance with the NFL measurements. P.B.M. is supported by Great Ormond Street Children's Charity (GOSHCC) and by the National Institute for Health Research Biomedical Research Centre at GOSH for Children NHS Foundation Trust and University College London. We thank M. Corbett and J. Hardy for valuable discussions and comments on the manuscript.

Author contributions

VC, HH, NWW, JER, PTC, PBM, KMB, JWC contributed to conception and design of the study. VC, MPW, JWC, JV, MNZ, EZP, SE, SP, MRC, GA, YTL, ET, NAH, JAB, MR, PN, AM, KC, KK, AE, MO, YI, PB, JECJ, OB, FB, CC, MMR, MF, AH, HZ, SJRH, NWW, JER, KMB, PBM, PTC, HH contributed to acquisition and analysis of data. VC, HH, PTC, PBM, MW, MRC, GA, KMB, JWC contributed to drafting the text and preparing the figures.

Conflict of Interest. The authors declare no competing conflict of interest.

References

1. Gess, B., Baets, J., De Jonghe, P., Reilly, M.M., Pareyson, D., and Young, P. (2015). Ascorbic acid for the treatment of Charcot-Marie-Tooth disease. The Cochrane database of systematic reviews, Cd011952.
2. d'Ydewalle, C., Benoy, V., and Van Den Bosch, L. (2012). Charcot-Marie-Tooth disease: emerging mechanisms and therapies. The international journal of biochemistry & cell biology 44, 1299-1304.
3. Zuchner, S., and Vance, J.M. (2006). Mechanisms of disease: a molecular genetic update on hereditary axonal neuropathies. Nature clinical practice Neurology 2, 45-53.
4. Braathen, G.J., Sand, J.C., Lobato, A., Hoyer, H., and Russell, M.B. (2011). Genetic epidemiology of Charcot-Marie-Tooth in the general population. European journal of neurology 18, 39-48.
5. Skre, H. (1974). Genetic and clinical aspects of Charcot-Marie-Tooth's disease. Clinical genetics 6, 98-118.
6. Nicolaou, P., Zamba-Papanicolaou, E., Koutsou, P., Kleopa, K.A., Georghiou, A., Hadjigeorgiou, G., Papadimitriou, A., Kyriakides, T., and Christodoulou, K. (2010). Charcot-Marie-Tooth disease in Cyprus: epidemiological, clinical and genetic characteristics. Neuroepidemiology 35, 171-177.
7. Nelis, E., Van Broeckhoven, C., De Jonghe, P., Lofgren, A., Vandenberghe, A., Latour, P., Le Guern, E., Brice, A., Mostacciuolo, M.L., Schiavon, F., et al. (1996). Estimation of the mutation frequencies in Charcot-Marie-Tooth disease type 1 and hereditary neuropathy with liability to pressure palsies: a European collaborative study. European journal of human genetics : EJHG 4, 25-33.
8. Morocutti, C., Colazza, G.B., Soldati, G., D'Alessio, C., Damiano, M., Casali, C., and Pierelli, F. (2002). Charcot-Marie-Tooth disease in Molise, a central-southern region of Italy: an epidemiological study. Neuroepidemiology 21, 241-245.
9. Murphy, S.M., Laura, M., Fawcett, K., Pandraud, A., Liu, Y.T., Davidson, G.L., Rossor, A.M., Polke, J.M., Castleman, V., Manji, H., et al. (2012). Charcot-Marie-Tooth disease: frequency of genetic subtypes and guidelines for genetic testing. Journal of neurology, neurosurgery, and psychiatry 83, 706-710.
10. Skinner, A., and Turner-Stokes, L. (2006). The use of standardized outcome measures in rehabilitation centres in the UK. Clinical rehabilitation 20, 609-615.
11. Shy, M.E., Blake, J., Krajewski, K., Fuerst, D.R., Laura, M., Hahn, A.F., Li, J., Lewis, R.A., and Reilly, M. (2005). Reliability and validity of the CMT neuropathy score as a measure of disability. Neurology 64, 1209-1214.
12. Murphy, S.M., Herrmann, D.N., McDermott, M.P., Scherer, S.S., Shy, M.E., Reilly, M.M., and Pareyson, D. (2011). Reliability of the CMT neuropathy score (second version) in Charcot-Marie-Tooth disease. Journal of the peripheral nervous system : JPNS 16, 191-198.

13. Li, H., and Durbin, R. (2010). Fast and accurate long-read alignment with Burrows-Wheeler transform. Bioinformatics 26, 589-595.
14. McKenna, A., Hanna, M., Banks, E., Sivachenko, A., Cibulskis, K., Kernytsky, A., Garimella, K., Altshuler, D., Gabriel, S., Daly, M., et al. (2010). The Genome Analysis Toolkit: a MapReduce framework for analyzing next-generation DNA sequencing data. Genome Res 20, 1297-1303.
15. Van der Auwera, G.A., Carneiro, M.O., Hartl, C., Poplin, R., Del Angel, G., Levy-Moonshine, A., Jordan, T., Shakir, K., Roazen, D., Thibault, J., et al. (2013). From FastQ data to high confidence variant calls: the Genome Analysis Toolkit best practices pipeline. Curr Protoc Bioinformatics 43, 11 10 11-33.
16. DePristo, M.A., Banks, E., Poplin, R., Garimella, K.V., Maguire, J.R., Hartl, C., Philippakis, A.A., del Angel, G., Rivas, M.A., Hanna, M., et al. (2011). A framework for variation discovery and genotyping using next-generation DNA sequencing data. Nat Genet 43, 491-498.
17. Danecek, P., and McCarthy, S.A. (2017). BCFtools/csq: Haplotype-aware variant consequences. Bioinformatics (Oxford, England).
18. Yang, H., and Wang, K. (2015). Genomic variant annotation and prioritization with ANNOVAR and wANNOVAR. Nature protocols 10, 1556-1566.
19. Seelow, D., Schuelke, M., Hildebrandt, F., and Nurnberg, P. (2009). HomozygosityMapper--an interactive approach to homozygosity mapping. Nucleic Acids Res 37, W593-599.
20. Narasimhan, V., Danecek, P., Scally, A., Xue, Y., Tyler-Smith, C., and Durbin, R. (2016). BCFtools/RoH: a hidden Markov model approach for detecting autozygosity from next-generation sequencing data. Bioinformatics (Oxford, England) 32, 1749-1751.
21. Genomes Project, C., Auton, A., Brooks, L.D., Durbin, R.M., Garrison, E.P., Kang, H.M., Korbel, J.O., Marchini, J.L., McCarthy, S., McVean, G.A., et al. (2015). A global reference for human genetic variation. Nature 526, 68-74.
22. Exome Variant Server, NHLBI GO Exome Sequencing Project (ESP), Seattle, WA. In. (
23. Lek, M., Karczewski, K.J., Minikel, E.V., Samocha, K.E., Banks, E., Fennell, T., O'Donnell-Luria, A.H., Ware, J.S., Hill, A.J., Cummings, B.B., et al. (2016). Analysis of protein-coding genetic variation in 60,706 humans. Nature 536, 285-291.
24. Beaulieu, C.L., Majewski, J., Schwartzentruber, J., Samuels, M.E., Fernandez, B.A., Bernier, F.P., Brudno, M., Knoppers, B., Marcadier, J., Dyment, D., et al. (2014). FORGE Canada Consortium: outcomes of a 2-year national rare-disease gene-discovery project. American journal of human genetics 94, 809-817.
25. (2015). Human genomics. The Genotype-Tissue Expression (GTEx) pilot analysis: multitissue gene regulation in humans. Science (New York, NY) 348, 648-660.
26. Johnson, W.E., Li, C., and Rabinovic, A. (2007). Adjusting batch effects in microarray expression data using empirical Bayes methods. Biostatistics (Oxford, England) 8, 118-127.

27. Langfelder, P., and Horvath, S. (2008). WGCNA: an R package for weighted correlation network analysis. BMC bioinformatics 9, 559.
28. Botia, J.A., Vandrovcova, J., Forabosco, P., Guelfi, S., D'Sa, K., Hardy, J., Lewis, C.M., Ryten, M., and Weale, M.E. (2017). An additional k-means clustering step improves the biological features of WGCNA gene co-expression networks. BMC systems biology 11, 47.
29. Reimand, J., Kull, M., Peterson, H., Hansen, J., and Vilo, J. (2007). g:Profiler--a web-based toolset for functional profiling of gene lists from large-scale experiments. Nucleic acids research 35, W193-200.
30. Shannon, P., Markiel, A., Ozier, O., Baliga, N.S., Wang, J.T., Ramage, D., Amin, N., Schwikowski, B., and Ideker, T. (2003). Cytoscape: a software environment for integrated models of biomolecular interaction networks. Genome research 13, 2498-2504.
31. Malik, K. (1997). Chemometric and Quantum Mechanical Methods for Analysing CD spectra. In. (London London: University of London.
32. Gorry, P.A. (1990). General least-squares smoothing and differentiation by the convolution (Savitzky-Golay) method. Analytical Chemistry 62, 570-573.
33. Hands-Taylor, K.L., Martino, L., Tata, R., Babon, J.J., Bui, T.T., Drake, A.F., Beavil, R.L., Pruijn, G.J., Brown, P.R., and Conte, M.R. (2010). Heterodimerization of the human RNase P/MRP subunits Rpp20 and Rpp25 is a prerequisite for interaction with the P3 arm of RNase MRP RNA. Nucleic acids research 38, 4052-4066.
34. Romero-Calvo, I., Ocon, B., Martinez-Moya, P., Suarez, M.D., Zarzuelo, A., Martinez-Augustin, O., and de Medina, F.S. (2010). Reversible Ponceau staining as a loading control alternative to actin in Western blots. Analytical biochemistry 401, 318-320.
35. Wilson, M.P., Footitt, E.J., Papandreou, A., Uudelepp, M.L., Pressler, R., Stevenson, D.C., Gabriel, C., McSweeney, M., Baggot, M., Burke, D., et al. (2017). An LC-MS/MS-Based Method for the Quantification of Pyridox(am)ine 5'-Phosphate Oxidase Activity in Dried Blood Spots from Patients with Epilepsy. Analytical Chemistry 89, 8892-8900.
36. Scott, T.A., Quintaneiro, L.M., Norvaisas, P., Lui, P.P., Wilson, M.P., Leung, K.Y., Herrera-Dominguez, L., Sudiwala, S., Pessia, A., Clayton, P.T., et al. (2017). Host-Microbe Co-metabolism Dictates Cancer Drug Efficacy in C. elegans. Cell 169, 442-456.e418.
37. Chalmers, R.M., Riordan-Eva, P., and Wood, N.W. (1997). Autosomal recessive inheritance of hereditary motor and sensory neuropathy with optic atrophy. Journal of neurology, neurosurgery, and psychiatry 62, 385-387.
38. Zeisel, A., Hochgerner, H., Lonnerberg, P., Johnsson, A., Memic, F., van der Zwan, J., Haring, M., Braun, E., Borm, L., La Manno, G., et al. (2018). Molecular architecture of the mouse nervous system. bioRxiv.
39. Musayev, F.N., di Salvo, M.L., Ko, T.P., Gandhi, A.K., Goswami, A., Schirch, V., and Safo, M.K. (2007). Crystal Structure of human pyridoxal kinase: structural basis of

M(+) and M(2+) activation. Protein science : a publication of the Protein Society 16, 2184-2194.

40. Gandhi, A.K., Desai, J.V., Ghatge, M.S., di Salvo, M.L., Di Biase, S., Danso-Danquah, R., Musayev, F.N., Contestabile, R., Schirch, V., and Safo, M.K. (2012). Crystal structures of human pyridoxal kinase in complex with the neurotoxins, ginkgotoxin and theophylline: insights into pyridoxal kinase inhibition. PloS one 7, e40954.
41. Kelly, S.M., Jess, T.J., and Price, N.C. (2005). How to study proteins by circular dichroism. Biochimica et biophysica acta 1751, 119-139.
42. Flanagan, J.M., and Beutler, E. (2006). The genetic basis of human erythrocyte pyridoxal kinase activity variation. Haematologica 91, 801-804.
43. Gisslen, M., Price, R.W., Andreasson, U., Norgren, N., Nilsson, S., Hagberg, L., Fuchs, D., Spudich, S., Blennow, K., and Zetterberg, H. (2016). Plasma Concentration of the Neurofilament Light Protein (NFL) is a Biomarker of CNS Injury in HIV Infection: A Cross-Sectional Study. EBioMedicine 3, 135-140.
44. Sandelius, A., Zetterberg, H., Blennow, K., Adiutori, R., Malaspina, A., Laura, M., Reilly, M.M., and Rossor, A.M. (2018). Plasma neurofilament light chain concentration in the inherited peripheral neuropathies. Neurology 90, e518-e524.
45. Vrolijk, M.F., Opperhuizen, A., Jansen, E., Hageman, G.J., Bast, A., and Haenen, G. (2017). The vitamin B6 paradox: Supplementation with high concentrations of pyridoxine leads to decreased vitamin B6 function. Toxicology in vitro : an international journal published in association with BIBRA 44, 206-212.
46. Mills, P.B., Surtees, R.A., Champion, M.P., Beesley, C.E., Dalton, N., Scambler, P.J., Heales, S.J., Briddon, A., Scheimberg, I., Hoffmann, G.F., et al. (2005). Neonatal epileptic encephalopathy caused by mutations in the PNPO gene encoding pyridox(am)ine 5'-phosphate oxidase. Human molecular genetics 14, 1077-1086.
47. Mills, P.B., Struys, E., Jakobs, C., Plecko, B., Baxter, P., Baumgartner, M., Willemsen, M.A., Omran, H., Tacke, U., Uhlenberg, B., et al. (2006). Mutations in antiquitin in individuals with pyridoxine-dependent seizures. Nature medicine 12, 307-309.
48. Pena, I.A., Roussel, Y., Daniel, K., Mongeon, K., Johnstone, D., Weinschutz Mendes, H., Bosma, M., Saxena, V., Lepage, N., Chakraborty, P., et al. (2017). Pyridoxine-Dependent Epilepsy in Zebrafish Caused by Aldh7a1 Deficiency. Genetics 207, 1501-1518.
49. Darin, N., Reid, E., Prunetti, L., Samuelsson, L., Husain, R.A., Wilson, M., El Yacoubi, B., Footitt, E., Chong, W.K., Wilson, L.C., et al. (2016). Mutations in PROSC Disrupt Cellular Pyridoxal Phosphate Homeostasis and Cause Vitamin-B6-Dependent Epilepsy. American journal of human genetics 99, 1325-1337.
50. Johnstone, D.L., Al-Shekaili, H.H., Tarailo-Graovac, M., Wolf, N.I., Ivy, A.S., Demarest, S., Roussel, Y., Ciapaite, J., van Roermund, C.W.T., Kernohan, K.D., et al. (2019). PLPHP deficiency: clinical, genetic, biochemical, and mechanistic insights. Brain : a journal of neurology 142, 542-559.

51. Meisler, N.T., and Thanassi, J.W. (1980). Pyridoxine kinase, pyridoxine phosphate phosphatase and pyridoxine phosphate oxidase activities in control and B-6-deficient rat liver and brain. The Journal of nutrition 110, 1965-1975.
52. Lumeng, L., Ryan, M.P., and Li, T.K. (1978). Validation of the diagnostic value of plasma pyridoxal 5'-phosphate measurements in vitamin B6 nutrition of the rat. The Journal of nutrition 108, 545-553.
53. Whittaker, J.W. (2016). Intracellular trafficking of the pyridoxal cofactor. Implications for health and metabolic disease. Archives of biochemistry and biophysics 592, 20-26.
54. Wong, H.H., Lin, J.Q., Strohl, F., Roque, C.G., Cioni, J.M., Cagnetta, R., Turner-Bridger, B., Laine, R.F., Harris, W.A., Kaminski, C.F., et al. (2017). RNA Docking and Local Translation Regulate Site-Specific Axon Remodeling In Vivo. Neuron 95, 852-868.e858.
55. Cioni, J.M., Koppers, M., and Holt, C.E. (2018). Molecular control of local translation in axon development and maintenance. Current opinion in neurobiology 51, 86-94.
56. Shigeoka, T., Jung, H., Jung, J., Turner-Bridger, B., Ohk, J., Lin, J.Q., Amieux, P.S., and Holt, C.E. (2016). Dynamic Axonal Translation in Developing and Mature Visual Circuits. Cell 166, 181-192.
57. Xu, W.Y., Gu, M.M., Sun, L.H., Guo, W.T., Zhu, H.B., Ma, J.F., Yuan, W.T., Kuang, Y., Ji, B.J., Wu, X.L., et al. (2012). A nonsense mutation in DHTKD1 causes Charcot-Marie-Tooth disease type 2 in a large Chinese pedigree. American journal of human genetics 91, 1088-1094.
58. Xu, W., Zhu, H., Gu, M., Luo, Q., Ding, J., Yao, Y., Chen, F., and Wang, Z. (2013). DHTKD1 is essential for mitochondrial biogenesis and function maintenance. FEBS letters 587, 3587-3592.
59. Gilman, S. (2002). Joint position sense and vibration sense: anatomical organisation and assessment. Journal of neurology, neurosurgery, and psychiatry 73, 473-477.
60. di Salvo, M.L., Contestabile, R., and Safo, M.K. (2011). Vitamin B(6) salvage enzymes: mechanism, structure and regulation. Biochimica et biophysica acta 1814, 1597-1608.
61. di Salvo, M.L., Safo, M.K., and Contestabile, R. (2012). Biomedical aspects of pyridoxal 5'-phosphate availability. Frontiers in bioscience (Elite edition) 4, 897-913.
62. Clayton, P.T. (2006). B6-responsive disorders: a model of vitamin dependency. Journal of inherited metabolic disease 29, 317-326.
63. Gandhi, A.K., Ghatge, M.S., Musayev, F.N., Sease, A., Aboagye, S.O., di Salvo, M.L., Schirch, V., and Safo, M.K. (2009). Kinetic and structural studies of the role of the active site residue Asp235 of human pyridoxal kinase. Biochemical and biophysical research communications 381, 12-15.
64. Albersen, M., Bosma, M., Luykx, J.J., Jans, J.J., Bakker, S.C., Strengman, E., Borgdorff, P.J., Keijzers, P.J., van Dongen, E.P., Bruins, P., et al. (2014). Vitamin B-6 vitamers

in human plasma and cerebrospinal fluid. The American journal of clinical nutrition 100, 587-592.

FIGURE LEGEND

Figure 1. Bi-allelic *PDXK* mutations are associated with axonal polyneuropathy and optic atrophy.

A. Pedigree of the two families with *PDXK* mutations.

B. Phenotype of the cases with *PDXK* mutations presenting with muscle atrophy of the intrinsic muscles of the hands with clawing of the hands, thin wrists, *pes cavus* and muscle atrophy in the feet and calves (B1-B3 from case F1-II-5, B4-B6 case F1-II-6).

C. Fundoscopy confirmed bilateral optic disc atrophy in both cases (C1 for F1-II-5 and C2 in F1-II-6).

D. Nerve biopsy from case F1-II-6 showing axonopathy. There is diffuse and severe depletion of both small and large myelinated axons with most of the surviving axons being less than 5µm in diameter. There were no axonal ovoids but there were regenerating clusters (arrows) consistent with long standing indolent axonopathy. There is no demyelination process.

E. Sanger sequencing confirming the homozygous c.682G>A mutation in two affected siblings and heterozygous state in unaffected family member in family 1 and homozygous c.659G>A in the two affected siblings and segregation in family 2.

F. Vitamin B_6 metabolic pathway. Phosphorylated B_6 vitamers (PMP; pyridoxamine 5'-phosphate, PNP; pyridoxine 5'-phosphate, PLP; pyridoxal 5'-phosphate) present in the diet are hydrolysed to pyridoxal (PL), pyridoxamine (PM) and pyridoxine (PN) by intestinal phosphatases prior to absorption and then converted to their 5'-phosphate derivatives in

the liver by pyridoxal kinase (PDXK). PNP and PMP are then converted to PLP, by pyridox(am)ine 5'-phosphate oxidase (PNPO). PLP re-enters the circulation bound to a lysine residue of albumin. Homeostatic regulation of tissue levels of PLP is achieved by various mechanisms, including feedback inhibition of PNPO and pyridoxal kinase by PLP[60]. Albumin in plasma, haemoglobin in erthyrocytes and glycogen phosphorylase in muscle also play a role, binding to PLP and helping to keep concentrations of this very reactive aldehyde low[61] so as to avoid any unwanted reactions with biologically important molecules. Subsequent delivery of PLP to the tissues requires hydrolysis of circulating PLP to pyridoxal by the ecto-enzyme tissue nonspecific alkaline phosphatase (TNSALP). The resulting pyridoxal is able to enter cells prior to being re-phosphorylated by pyridoxal kinase to produce the active cofactor, PLP, required by B_6-dependent apoenzymes[62]. Within cells, recycling pathways also exist with PMP being oxidised by PNPO to form PLP[61].

Figure 2. *PDXK* is highly expressed in peripheral and central nervous systems and in the same regulon with genes already linked to axonal peripheral neuropathies.

A. Expression of *PDXK* in human tissues. Box and whisker plots showing the expression of *PDXK* across multiple human tissues. Data generated by the GTEx consortium. Expression in tibial nerve is highlighted with a dark grey arrow and is amongst the tissues with the highest *PDXK* expression.

B. Expression of *PDXK* in multiple cell types of the mouse central and peripheral nervous system generated using single cell RNA-seq. *PDXK* gene expression across single cells isolated from the mouse central and peripheral nervous system and displayed using a heatmap demonstrates highest expression of this gene in neurons of the mouse hindbrain[38] with expression in the peripheral neurons including sensory neurons.

C. Top Down plot of the black module genes in the tibial nerve tissue. Only the most connected genes are shown. *PDXK* gene is highlighted in yellow. Genes known to be associated with GO term GO:0055114, oxidation-reduction process are highlighted in red. Size of gene nodes reflects their connectivity with the rest of genes in the module. PDXK is amongst the top 60 most connected genes. Proximity of genes in the plot reflects their similarity in terms of shared connections with other genes. Interestingly, within the *PDXK* regulon from the tibial nerve we found *DHTKD1* already linked to Mendelian disorders and associated with primary peripheral axonal neuropathy[57; 58].

D. Conservation of p. Ala228Thr and p.Arg220Gln in *PDXK* across species.

E. Crystal structure of human pyridoxal kinase with bound ATP (PBS accession 3KEU). PDXK is a dimeric enzyme with one active site per monomer[63] (monomers A and B are depicted in green and yellow, respectively). In the PDXK structure, the backbone-carbonyl oxygen of Alanine 228 establishes a hydrogen bond with the adenine NH_2 group of ATP. The active site of each monomer binds one ATP molecule, two Mg^{2+} ions and one Na^{2+} ion. The ATP binding site is composed of a β-loop-β structure, often referred as a flap, which provides numerous hydrogen-bond interactions to the ATP β- and γ-phosphates, and sequesters the ATP for catalysis.[39] Arginine 220 is located in the β9, in the vicinity of ATP binding site.

Figure 3. *PDXK* mutations lead to reduced pyridoxal kinase enzymatic activity and low PLP.

A. Circular dichroism analyses of recombinant PDXK WT and p.Ala228Thr mutant proteins. The left and right panels show the normalised far-UV and near-UV spectra of the two proteins, respectively. A clear difference in secondary structure content between the two proteins is observed from the far-UV experiment.

B. Analysis of the interaction of non-hydrolysable analogue ATPγS with PDXK WT and p.Ala228Thr mutant proteins by ITC. The left panel shows the titration of ATPγS (250 μM) into a PDXK WT solution (25 μM). The thermogram shows that the interaction was entropically and enthalpically favoured, with ΔH -3.27 ± 0.42 kcal/mol, -TΔS -4.42 ± 0.48 kcal/mol, K_D 2.33 ± 0.25 μM and ΔG -7.69 ± 0.06 kcal/mol. The stoichiometry was 0.80 ± 0.02 μM, indicating that each molecule of PDXK binds to one molecule of ATPγS. The right panel reports the titration of ATPγS (250 μM) into a PDXK p.Ala228Thr solution (25 μM). The experiment showed no interaction under the experimental conditions tested, suggesting that the mutation affected the ability of the kinase to bind the analogue substrate ATPγS.

C. Western blot analysis shows normal expression of the PDXK protein in cases compared to controls. WT= wild-type.

D. Activity of recombinant wild-type and p.Ala228Thr pyridoxal kinase protein measured as pyridoxal 5'-phosphate formation. Conditions: 0 – 100 μmol L^{-1} pyridoxal (PL); 300 μmol L^{-1} MgATP; 20 mmol L^{-1} potassium phosphate, pH 7.0; 37°C; 10 min incubation with

100 ng recombinant protein. Points displayed are a mean of three repeats. V_{max}: WT = 2.17 µmol L^{-1} hr^{-1}; p.Ala228Thr = 2.52 µmol L^{-1} h^{-1}. K_m: WT = 14.53 µmol L^{-1}; p.Ala228Thr = 31.93 µmol L^{-1}.

E. Kinetics of recombinant wild-type and p.Ala228Thr pyridoxal kinase protein upon variation of pyridoxal concentration. Pyridoxal kinase activity of recombinant human WT and p.Ala228Thr PDXK protein is measured as PLP formed after incubation with the substrate PL. Incubations performed in the presence of variable concentrations of MgATP (0 – 500 µmol/L) and 50 µmol/L pyridoxal. Kinetics were sigmoidal and parameters established were as follows: WT $k_{0.5}$ = 53.4 µmol/L; V_{max} = 16.8 pmol h^{-1}, p.Ala228Thr $k_{0.5}$ = 174.4 µmol/L; V_{max}= 6.3 pmol h^{-1}. Results indicate a dramatic reduction in the catalytic efficiency of the p.Ala228Thr PDXK protein. n = 3 at each data point.

F. Erythrocyte PDXK activity in dried blood spots from cases homozygous for the p.Ala228Thr and p.Arg220Gln versus controls (ages 15–92). Patients homozygous for p.Ala228Thr and p.Arg220Gln have lower activity than all controls. Activity measured as PLP formed after incubation of a 3mm dried blood spot punch with pyridoxal. Each sample was analysed in duplicate and the mean is shown. There was no correlation of PDXK activity with age.

G-H. Comparison of plasma PLP concentrations (retention time of 2.78/2.84 mins) in control (red) and cases carrying the *PDXK* mutation (blue) p.Arg220Gln (G) and p.Ala228Thr (H) show a significant reduction of PLP in the case samples (7.8 and 9 nmol/L respectively) vs control (control range 25-75 nmol/L).

Figure 4. PLP supplementation in patients with *PDXK* mutations can rescue the biochemical phenotype.

A. Concentrations of plasma B_6 vitamers in affected homozygous cases for p. Ala228Thr (F1-II-5), p.Arg220Gln (F2-II-2) and a heterozygous (F1-III-1) *PDXK* mutation carrier. The levels prior to supplementation were compared to published range of B_6 vitamers in adult controls (n=523)[64] not receiving PLP. PL, pyridoxal; PN, pyridoxine; PM, pyridoxamine; PLP, pyridoxal 5'-phosphate; PNP, pyridoxine 5'-phosphate; PMP, pyridoxamine 5'-phosphate; PA, 4-pyridoxic acid. All units nmol/L, except for PNP which is stated in 'concentration units'. n.d, not detected; RI, reference interval; hom, homozygous; het-heterozygous.

B. The effect of PLP supplementation on plasma PLP concentrations of a case with *PDXK* mutations. The red bar represents the PLP levels in a group of adult controls with no B_6 supplementation. There is a significant difference in the plasma PLP concentration of F1-II-5 before supplementation (blue bar) and on PLP replacement (magenta bar) (***; $p < 0.05$). The difference between groups was tested with the use of a one-way analysis-of-variance test followed by the Tukey-Kramer test. The horizontal lines on the bars indicate mean values ±1 SD.

C. Neurofilament light (NFL) concentrations in plasma from cases with homozygous p.Arg220Gln and p.Ala228Thr *PDXK* mutations and heterozygous carrier (F1-III-1). The blue bars show that NFL levels prior to PLP supplementation are high and consistent with values published in other inherited peripheral neuropathies[44] (solid line) indicating on-

going axonal damage. The orange, grey and yellow bars shows the NFL levels in the cases from family 1 at 4, 12 and 24 months on PLP supplementation respectively. The levels have reduced to that of normal controls (dashed line) and continued to improve with longitudinal follow-up suggesting an amelioration of the axonal breakdown.

Table legends

Table 1. Detailed description of the clinical phenotype associated with *PDXK* mutations.

Table 2. Plasma B_6 vitamer profiles for cases with PROSC, PNPO and PDXK deficiency supplemented with pyridoxal 5'-phosphate

Table 3. Vitamin B_6-related disease models

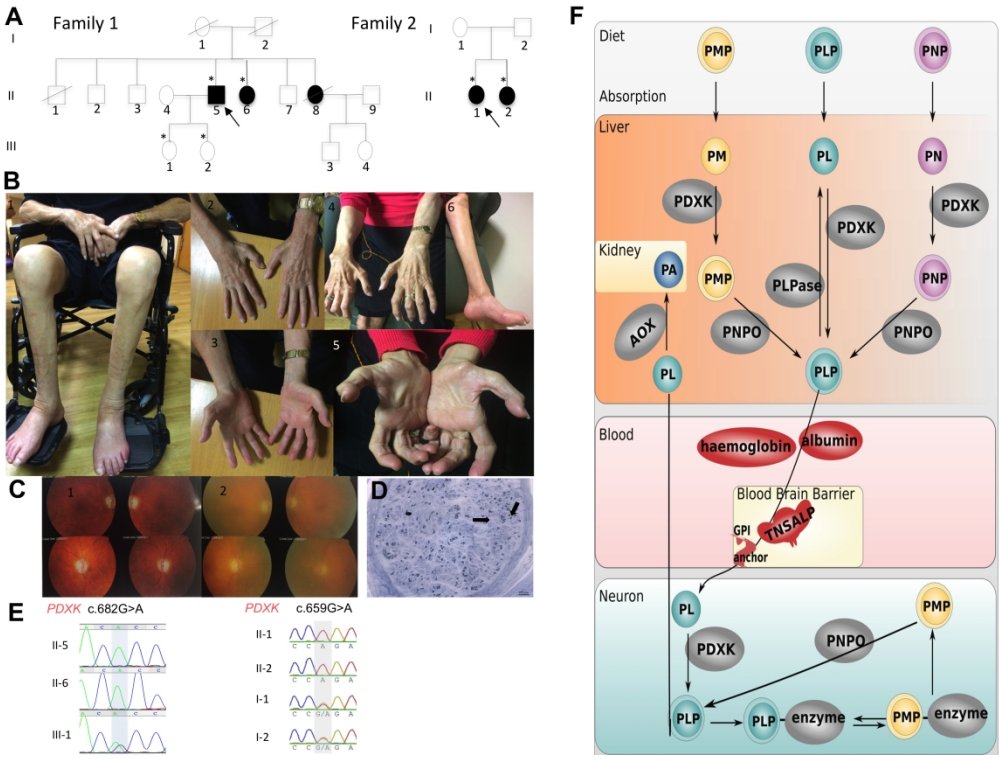

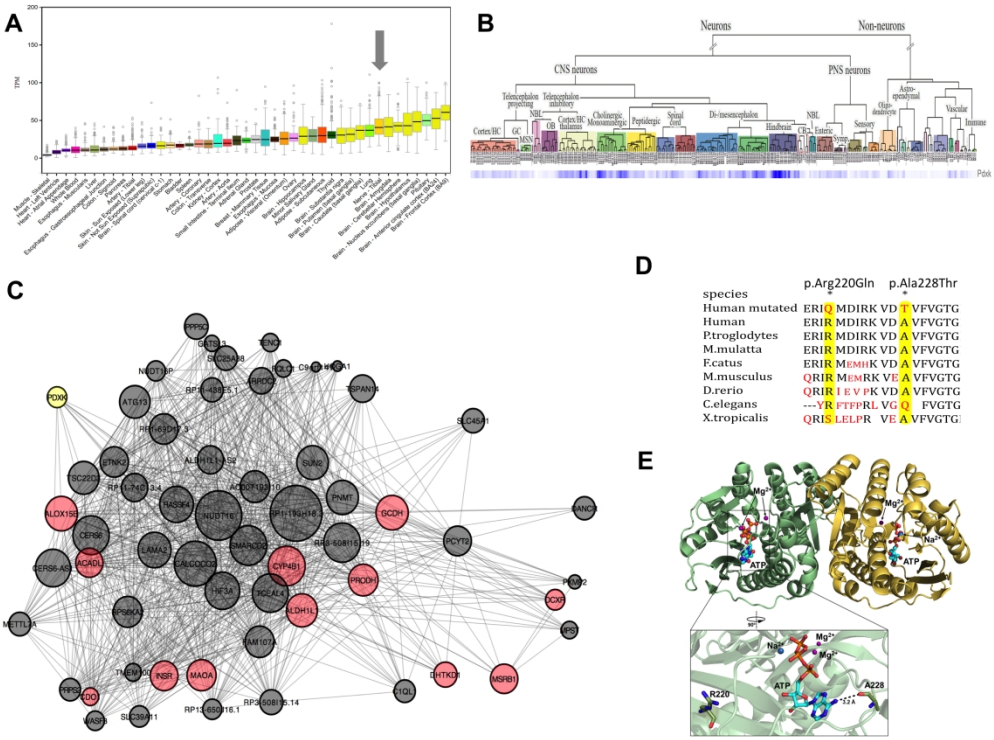

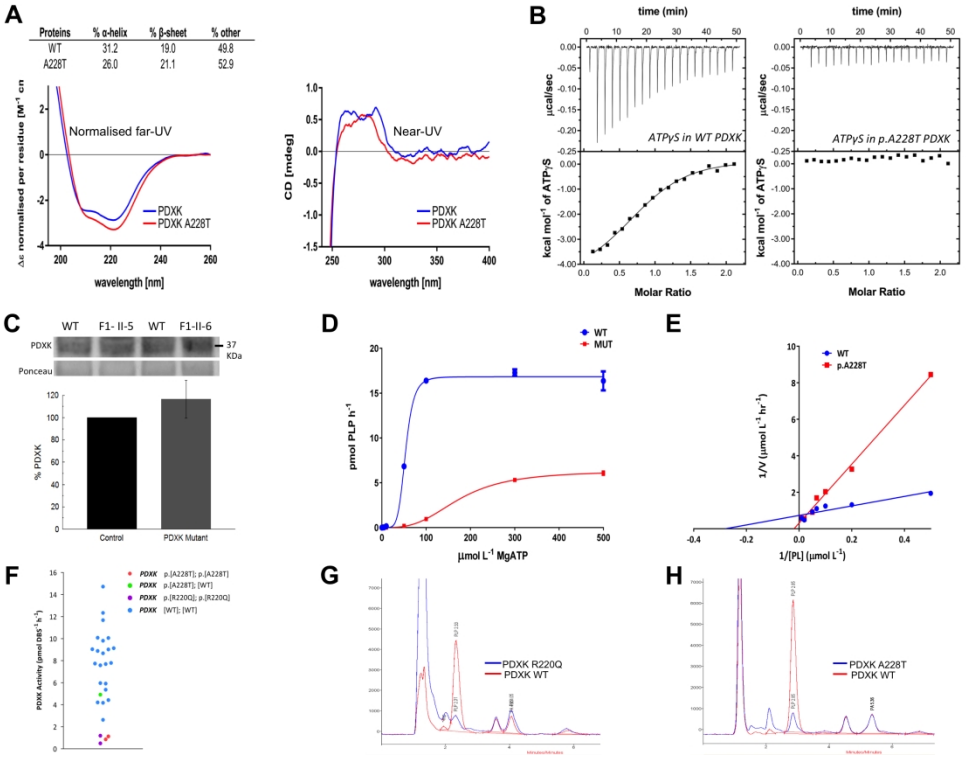

A

	Pre-treatment					On PLP replacement treatment			
	F1-II-5 *PDXK* p.Ala228Thr hom		F2-II-2 *PDXK* p.Arg220Gln hom	F1-III-1 *PDXK* p.Ala228Thr het	Reference range (95% RI)	F1-II-5 *PDXK* p.Ala228Thr			
B_6 vitamers (nmol/L)	-4 months	baseline	baseline			2 weeks	4 weeks	12 weeks	12 months
PLP	9	7.4	7.8	76	19.8 – 200	839	311	461	415
PL	9	6	17.6	24	4.2 – 24.5	443	413	824	1550
PN	nd	nd	nd	nd	nd	4689	14.9	nd	31.3
PM	nd	nd	nd	nd	nd	nd	nd	3.3	nd
PA	17	12	22.4	20	6.1 – 107	1493	877.4	1524	1617

B

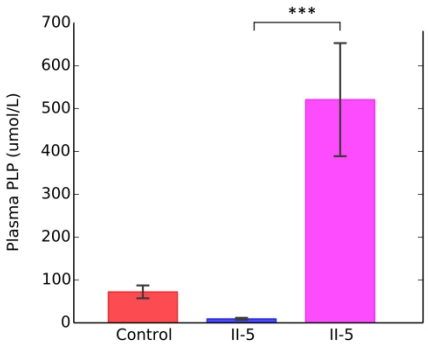

C

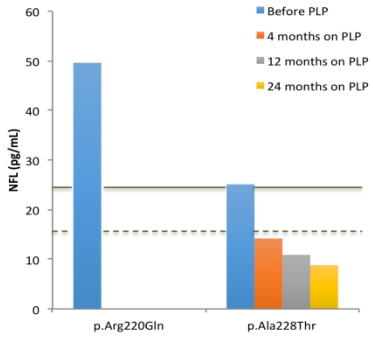

Table 1. Detailed phenotype of the affected cases carrying *PDXK* mutations

	Phenotype/case	F1-II-5	F1-II-6	F1-II-8	F2-II-1	F2-II-2
Demographics	Gender	Male	Female	Female	Female	Female
	Age at examination (in years)	79	74	Died at 71 from leukaemia	31	29
	Age at onset (in years)	7	9	7	5	2
Progression	Symptoms at onset	Lower limb weakness and wasting				
	Upper limb weakness	At 12 years	At 12 years	At 17 years	20s	20s
	Optic atrophy	At 40 years	At 47 years	At 50 years	31	29
Neurological examination	Fundoscopy	Pale optic discs bilaterally	Pale optic discs bilaterally	NA	Mild optic disc pallor bilaterally	Mild optic disc pallor bilaterally
	Other cranial nerves	Normal				
	Skeletal deformities	*Pes cavus*, hammer toes, clawing of hands			*Pes cavus*, hammer toes	
	Power	Severe weakness of dorsi/plantar flexion, long finger extensors and intrinsic muscles of the hands			Moderate-severe weakness of dorsi/plantar flexion, long finger extensors and mild weakness of intrinsic muscles of the hands	
	MRC power score	44	44	NA	56	54
	Reflexes	Absent throughout. Mute plantar responses			Areflexia. Mute plantar responses	Areflexia. Mute plantar responses
	Sensation	Reduced pain to mid calf and wrists	Reduced pain to ankles and elbows		Reduced pain to ankles	Reduced pain to upper calf and base of fingers
		Reduced vibration sense to iliac crest and wrist	Reduced vibration sense to iliac crest and elbow		Vibration decreased to the knees	Vibration decreased to the knees
	Romberg's sign	Present	Present		Present	Present
	Coordination	Normal	Normal		Normal	Normal
	Visual acuities	Unable to count fingers	6/12 in both eyes		NA	NA
	Colour vision	Unable to distinguish any colour	Grossly impaired, 3/17 Ishihara plates		15/17 Ishihara plates	3/17 Ishihara plates
	Peripheral vision	Normal	Normal		Normal	Normal
	Cognitive function	Normal	Normal		Normal	Normal
	Seizures	Absent	Absent		Absent	Absent
Investigation results	MRI head	Normal	Normal		NA	NA
	Optic nerve and chiasm CT	Normal	Normal		NA	NA
	Visual evoked potentials (VEP)	Severely attenuated bilaterally with anomalous waveform on flash VEP.			NA	NA
	Somatosensory evoked potentials	NA	Poorly formed due to severe polyneuropathy		NA	NA
	Nerve conduction study	Severe sensori-motor axonal neuropathy	Severe sensori-motor axonal neuropathy		Severe sensori-motor axonal neuropathy	Severe sensori-motor axonal neuropathy
	Electromyography	Chronic denervation in a length dependent pattern. No myopathic changes.			Chronic denervation in a length dependent pattern. No myopathic changes.	
Biochemical profile	Renal function	Normal	Normal		Normal	Normal
	Liver function	Normal	Normal		Normal	Normal
	GI tract	Normal colonoscopy	Normal		Normal	Normal
	Plasma amino acids	Normal	NA		NA	NA
	Vitamin B_1 (normal range 67-265 nmol/L)	NA	176		149	183
	Vitamin B_9 (normal range 3.9-20 ng/mL)	Normal	NA		Normal	Normal
	Vitamin B_{12} (normal range 197-771 pg/mL)	938	454		293	211

Legend: NA- not available, GI- gastrointestinal, na-not available, PLP- pyridoxal phosphate. Plasma amino acids tested: methionine, isoleucine, leucine, tyrosine, phenylalanine, ornithine, lysine, histidine, and arginine.

Table 2. Plasma B_6 vitamer profiles for patients with PROSC, PNPO and PDXK deficiency supplemented with pyridoxal 5'-phosphate.

	Age	B_6 [dose]	PLP	PL	PA	PN	PNP	PMP	PM
Control range*	4.3 y – 16 y	None	46 - 321	5 - 18	16 - 139	nd - 0.6	nd	nd - 9	nd
PROSC**	3 y	PLP [70 mg QDS]	**2769**	**796**	**2043**	0.5	nd	nd	nd
PROSC**	6 m	PLP [45 mg/kg/day]	**2166**	**1695**	**700**	nd	nd	nd	nd
PNPO***	2 y	PLP [30 mg/kg/d]	**580**	**427**	**793**	**575**	**43**	**18**	**193**
PNPO***	10 y	PLP [30 mg/kg/d]	**633**	**5798**	**7926**	**599**	**77**	**101**	**2731**
PDXK****	79 y	PLP [50 mg/d]	**415**	**1550**	**1617**	**31**	**nd**	**nd**	**nd**

Legend: nd; not detected. PL, pyridoxal; PN, pyridoxine; PM, pyridoxamine; PLP, pyridoxal 5'-phosphate; PNP, pyridoxine 5'-phosphate; PMP, pyridoxamine 5'-phosphate; PA, 4-pyridoxic acid. All units nmol/L, except for PNP which is stated in 'concentration units'. Values outside the reference range are shown in bold. QDS = four times a day. *Control range as described in Footitt *et al.*, 2013; ** Data from Darin et al., 2017. ***Data from Footitt *et al.*, 2013. PLP doses received by PROSC and PNPO patients larger than the doses given to the PK-deficient patients (II-5 and II-6). ****Values at 12 months on treatment with PLP.

Table 3. Vitamin B_6-related disease models

Model	Phenotype	Mechanism	Effect on B_6 pathway	Response to PLP supplementation
Pharmacological models				
Isoniazid, levodopa, gentamicin, D-penicillamine	Axonal peripheral neuropathy[1]	Interaction between the reactive aldehyde group of PLP with nucleophilic acceptors such as amine, hydrazine, hydroxylamine or sulphydryl groups rendering PLP inactive	Decrease in serum PLP	Prevents onset of peripheral neuropathy
Methylxanthines	Axonal peripheral neuropathy[2; 3]	Directly inhibit enzymes involved in B_6 metabolism		
Carbamazepine, vigabatrin, sodium valproate	Axonal peripheral neuropathy[4 5-7]	Potent hepatic inducers of cytochrome P450, induce enzymes involved in the catabolism of PLP		
B_6 antivitamin Ginkgotoxin (4'-O-methylpyridoxine)	Epileptic convulsions, leg paralysis and loss of consciousness[8]	Analogue of PLP. Inhibition of pyridoxal kinase by serving as an alternate substrate for the enzyme	Decrease in PLP formation	NA
Animal models				
Mouse	Preweaning lethality (MGI:1351869)	*PDXK* knockout	NA	NA
Mouse	Abnormal walking track patterns, axonal peripheral neuropathy with intact myelin on nerve biopsy[9]	PLP dietary-deficient	Decrease in serum PLP	Complete reversal of symptoms with PLP supplementation
Rat	Tissue-specific PDXK response to B_6 deficiency [10; 11]	B_6 diet deficient	PDXK activity rapidly decreases in the liver, muscle and plasma compared to the brain	Reversal with PLP supplementation
C. elegans	Sensory-motor integration deficit in neuromuscular behaviour [12]	*PDXK* knockout	NA	Rescued by expression of a WT transgene.
Drosophila	Motility and eye dysfunction with compromised climbing ability, ommatidial array disruption and decreased longevity[13]	*PDXK* knockdown by RNA interference	NA	Rescued by expression of a WT transgene.